Unclassified
SECURITY CLASSIFICATION OF THIS PAGE

AD-A237 240

REPORT D

1a REPORT SECURITY CLASSIFICATION Unclassified	
2a SECURITY CLASSIFICATION AUTHORITY	3 DISTRIBUTION/AVAILABILITY OF REPORT Approved for public release: Distribution unlimited
2b DECLASSIFICATION/DOWNGRADING SCHEDULE	
4 PERFORMING ORGANIZATION REPORT NUMBER(S) 29	5 MONITORING ORGANIZATION REPORT NUMBER(S) 29
6a NAME OF PERFORMING ORGANIZATION Department of Chemistry University of California, Irvine	6b OFFICE SYMBOL (If applicable)
6c ADDRESS (City, State, and ZIP Code) Irvine, California 92717	7a NAME OF MONITORING ORGANIZATION University of California Contracts & Grants Administration
	7b ADDRESS (City, State, and ZIP Code) 113 Administration Building Irvine, California 92717
8a NAME OF FUNDING/SPONSORING ORGANIZATION Office of Naval Research	8b OFFICE SYMBOL (If applicable)
8c ADDRESS (City, State, and ZIP Code) Chemistry Division, Code: 1113PS 800 N. Quincy Street Arlington, VA 22217-5000	9 PROCUREMENT INSTRUMENT IDENTIFICATION NUMBER N00014-90-J-1180
	10 SOURCE OF FUNDING NUMBERS PROGRAM ELEMENT NO: 413q003--01 / PROJECT NO / TASK NO / WORK UNIT ACCESSION NO

11 TITLE (Include Security Classification)
A Vibrational Spectroscopy Study of CH_3COOH, CH_3COOD and $^{13}CD_3COOH(D)$ Adsorption on Pt(111): I. Surface Dimer Formation and Hydrogen Bonding

12 PERSONAL AUTHOR(S)
Quanyin Gao and John C. Hemminger

13a TYPE OF REPORT	13b TIME COVERED	14 DATE OF REPORT (Year, Month, Day)	15 PAGE COUNT
Interim/Technical	FROM _____ TO _____	91-06-01	32

16 SUPPLEMENTARY NOTATION
Surface Science, to be published.

17 COSATI CODES			18 SUBJECT TERMS (Continue on reverse if necessary and identify by block number)
FIELD	GROUP	SUB-GROUP	Acetic acid, Pt(111), vibrational spectroscopy, hydrogen bonding, dimers

19 ABSTRACT (Continue on reverse if necessary and identify by block number)

Acetic acid (CH_3COOH, CH_3COOD and $^{13}CD_3COOH(D)$) adsorption on Pt(111) at 168 K has been studied as a function of surface coverage with HREELS. At low acetic acid dosages (θ<0.3), dissociative adsorption occurs forming a surface acetate species with an $\eta^2_{(O,O)}$-CH_3COO configuration in a C_s symmetry. Further dissociative adsorption as $CO_{(a)}$, $O_{(a)}$ and $CH_{x(a)}$ with x=1-2 is observed for very low acetic acid dosages (θ~0.2 or less). The formation of $HCOO_{(a)}$ or $CH_{3(a)}$ from acetic acid adsorption is ruled out based on the absence of their characteristic vibrational modes. Molecular adsorption occurs at moderate acetic acid dosages (θ~0.5 or above) with a fingerprint peak at ~932cm^{-1} for CH_3COOH and $^{13}CD_3COOH$ adsorbates. This mode corresponds to a well documented γ_{OH} mode of the acetic acid dimer. Hydrogen bonding between neighboring acetic acid molecules is responsible for the stabilization of the acetic acid hydroxyl group. The adsorbed acetic acid configuration is proposed to be a cyclic dimer with the dimer ring nearly parallel to the plane of metal surface. Quantitative correlations have been developed between the frequency of the γ_{OH} mode and the strength (ΔH) and bond length ($R_{O\cdots O}$) of the hydrogen bond for a number of carboxylic acid dimers. Using these correlations from the literature our data can be used to estimate the hydrogen bond energy for acetic acid dimer on Pt(111) to be ~7.3kcal/mole with a corresponding estimate of the $R_{O\cdots O}$ distance of ~2.68Å.

20 DISTRIBUTION/AVAILABILITY OF ABSTRACT	21 ABSTRACT SECURITY CLASSIFICATION	
☒ UNCLASSIFIED/UNLIMITED ☐ SAME AS RPT ☐ DTIC USERS	Unclassified	
22a NAME OF RESPONSIBLE INDIVIDUAL John C. Hemminger	22b TELEPHONE (Include Area Code) (714) 856-6020	22c OFFICE SYMBOL

DD FORM 1473, 84 MAR — 83 APR edition may be used until exhausted. All other editions are obsolete.

SECURITY CLASSIFICATION OF THIS PAGE
Unclassified

OFFICE OF NAVAL RESEARCH

Contract N00014-90-J-1180

R&T Code 413q003----01

Technical Report No. 29

A Vibrational Spectroscopy Study of CH_3COOH, CH_3COOD and $^{13}CD_3COOH(D)$ Adsorption on Pt(111): I. Surface Dimer Formation and Hydrogen Bonding

by

Q. Gao and J.C. Hemminger

To be published in: Surface Science

University of California, Irvine
Institute for Surface and Interface Science, and
Department of Chemistry
Irvine, California

June 1, 1991

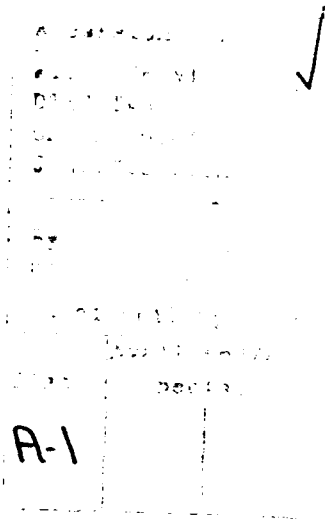

A Vibrational Spectroscopy Study of CH_3COOH, CH_3COOD and $^{13}CD_3COOH(D)$ Adsorption on Pt(111): I. Surface Dimer Formation And Hydrogen Bonding

Quanyin Gao and John C. Hemminger

Institute for Surface and Interface Science

and Department of Chemistry

University of California , Irvine

Irvine, CA 92717

To be published in: Surface Science

Abstract

Acetic acid (CH_3COOH, CH_3COOD and $^{13}CD_3COOH(D)$) adsorption on Pt(111) at 168K has been studied as a function of surface coverage with HREELS. At low acetic acid dosages ($\theta<0.3$), dissociative adsorption occurs forming a surface acetate species with an $\eta^2_{(O,O)}$-CH_3COO configuration in a C_s symmetry. Further dissociative adsorption as $CO_{(a)}$, $O_{(a)}$ and $CH_{x(a)}$ with x=1-2 is observed for very low acetic acid dosages (θ~0.2 or less). The formation of $HCOO_{(a)}$ or $CH_{3(a)}$ from acetic acid adsorption is ruled out based on the absence of their characteristic vibrational modes. Molecular adsorption occurs at moderate acetic acid dosages (θ~0.5 or above) with a finger print peak at ~932 cm^{-1} for CH_3COOH and $^{13}CD_3COOH$ adsorbates. This mode corresponds to a well documented γ_{OH} mode of the acetic acid dimer. Hydrogen bonding between neighboring acetic acid molecules is responsible for the stabilization of the acetic acid hydroxyl group. The adsorbed acetic acid configuration is proposed to be a cyclic dimer with the dimer ring nearly parallel to the plane of metal surface. Quantitative correlations have been developed between the frequency of the γ_{OH} mode and the strength (ΔH) and bond length ($R_{O....O}$) of the hydrogen bond for a number of carboxylic acid dimers. Using these correlations from the literature our data can be used to estimate the hydrogen bond energy for acetic acid dimer on Pt(111) to be ~7.3 kcal/mole with a corresponding estimate of the $R_{O....O}$ distance of ~2.68Å.

1. Introduction

Acetic acid has been known to form hydrogen bonded cyclic dimers in the gas phase [1]. In the liquid phase, both cyclic and chain types of dimers are considered possible while in the solid crystal, infinite chains of hydrogen bonded structure of acetic acid has been reported[2-3]. As a continued effort to study the hydrogen bonding effects on surface chemistry, acetic acid has been chosen here following our studies of formamide surface chemistry. For the latter, hydrogen bonding and its influence on surface chemistry has been investigated on both Ni(111)[4] and Pt(111)[5].

The adsorption of acetic acid on transition metal surfaces has been the subject of several previous experimental investigations [6-11]. On Pt(111), a previous study has shown acetate species formation by oxygen pre-adsorption on the surface at low temperature [6]. The acetate species has also been reported on Cu(100) [7-8] and Al(111)[11] at low acetic acid exposures. A hydrogen bonded dimer form of acetic acid has been observed on Al(111) at high exposure ($1.5x10^{17}$ molecules/cm^2), which is attributed to the physisorbed acetic acid molecules, from which we deduced that the adsorption is multilayer.

In our study, a systematic investigation is conducted to find the coverage dependence of hydrogen bonded species and the role it plays in surface chemistry. In order to have a clear vibrational mode assignments, isotopically labeled molecules of CH_3COOD and $^{13}CD_3COOH(D)$ are used in addition to CH_3COOH for the HREELS and TDS experiments.

2. Experimental section

The experiments were performed in a two level UHV chamber with a base pressure of $1x10^{-10}$ torr. The upper level is equipped with low energy electron diffraction (LEED) optics, Auger electron spectrometer with cylindrical mirror analyzer, quadrupole

mass spectrometer, ion sputtering gun and sample doser. The lower level houses the high resolution electron energy loss spectrometer (HREELS).

An LK2000-14-R HREEL spectrometer was used for the vibrational analysis with a routine resolution of about 30 cm^{-1} (FWHM of the elastic peak) for the clean Pt(111) surface. The spectral resolution did not degrade with acetic acid dosages within a monolayer coverage. A typical elastic beam counting rate at this resolution is about 10^5-10^6 counts/sec. From LEED measurements, no surface ordering was found for acetic acid adsorption on Pt(111) which indicates the high performance quality of the HREEL spectrometer given the system studied is a *disordered overlayer*. The incident electron beam energy used is about 7 volt and the incident angle is 60 degree from the surface normal of the Pt(111) sample. Unless mentioned otherwise in the figure, the spectra were recorded in the specular direction.

The Pt(111) surface was oriented to within $\pm 0.5^0$ of the desired (111) plane confirmed by both Laue X-ray diffraction and LEED. The surface cleanliness, following argon ion bombardments and oxygen treatments, was checked by both Auger electron spectroscopy (AES) and HREELS.

CH_3COOH, CH_3COOD and $^{13}CD_3COOH(D)$ were obtained from Aldrich. The purity of CH_3COOH is 99.7%. CH_3COOD has 98 atom% D isotope purity and $^{13}CD_3COOH(D)$ has 97.2 atom% ^{13}C, 97.27 atom% D for methyl group and 43 atom% D for hydroxyl group. They are further purified in the gas dosing line by several freeze-pump-thaw cycles. A doser was used for acetic acid adsorption onto the front face of the cooled Pt(111) crystal. The doser consists of a 1/4" O.D. stainless steel tube whose orifice was located approximately 1 cm from the crystal surface. Reproducing the acetic acid coverages was accomplished by immediately rotating the crystal out of the acetic acid dosing beam after the pre-set dosing time. The effectiveness of dosing in this manner was confirmed by monitoring the reproducibility of the HREELS and the thermal desorption spectroscopy (TDS).

3. Results

3.1 Adsorption of CH_3COOH on Pt(111) at 168K

A set of Auger peak to peak ratios of C_{273}/Pt_{237} were measured as a function of CH_3COOH dosage and the plot is shown in figure 1. This plot shows an abrupt change in slope at ~ 20 sec exposure time. The turning point for the slope change is assigned to monolayer exposure (θ=1) to establish a relative exposure scale. Our TDS results are consistent with this assignment which showed saturation exposure at this acetic acid dosage before the multilayer desorption peaks appear [12].

For the different CH_3COOH dosages shown in figure 1, corresponding HREEL spectra have been taken. Figure 2 is a plot of some of these HREEL spectra measured at 168K as a function of increasing CH_3COOH exposure. At initial small CH_3COOH dosage (θ~0.03) five vibrational modes are observed at 467, 661, 768, 1398 and 2057 cm^{-1}, as shown in figure 2a. After increasing the CH_3COOH dosage to θ~0.19, five more peaks occur at 302, 913, 1000, 2930 and 2988 cm^{-1} (figure 2b). Substantial peak broadening as a function of increasing dosage is observed for the band at about 2940 cm^{-1} (figure 2d-2h). At θ~0.30 dosage (figure 2c), the previous peak at 2048 cm^{-1} has disappeared accompanied by a drop of intensity of the 467 cm^{-1} peak, and a new peak is observed at 874 cm^{-1} (figure 2c) which later shifts to about 932 cm^{-1} with increasing coverage. A weak peak at 1660 cm^{-1} appears when CH_3COOH dosage is above θ~0.5 (figure 2d-2h). In figure 2f, a peak at 219 cm^{-1} is observed. With larger exposure, this peak is not detected which could be caused by the loss of resolution of this band with the tail of the elastic peak since the instrumental resolution decreases when large exposures are used (before figure 2f, FWHM is about 30 cm^{-1} for the elastic peak, after figure 2f, FWHM increases to ~ 40 cm^{-1}). In all spectra shown in figure 2, the dominant peak is at ~1400 cm^{-1}. The second dominant peak is at ~ 671 cm^{-1} for CH_3COOH dosages below θ~0.5.

When the acetic acid dosage exceeds θ~0.5 the peak at 932 cm^{-1} becomes the second dominant peak.

A series of CH_3COOH spectra with relative exposure of 7.5 measured at 168K are plotted out as a function of off-specular scattering angle (figure 3). At 10 degree off-specular (figure 3d), a peak splitting is observed clearly at 605 and 698, 910 and 1003, 1318 and 1400 cm^{-1} as well as a peak intensity enhancement for the 2927 cm^{-1} band. With small initial exposure of θ~0.19, the off-specular spectrum is shown in figure 4, in which only one peak splitting is observed at 1340 and 1400 cm^{-1} (figure 4b).

3.2 CH_3COOD adsorption on Pt(111) at 168K

Three exposures of CH_3COOD have been recorded and the HREEL spectra are shown in figure 5. At low exposure (θ~0.63), vibrational peaks are observed at 290, 464, 565, 680, 836, 942, 1029, 1156, 1388, 1660, 2038, 2910, 2979 and 3037 cm^{-1}(figure 5a), in which the dominant peak is at 1388 cm^{-1} and the second dominant peak is at 680 cm^{-1}. These two peaks change relative intensity at larger exposures as shown in figure 5b-5c where the 687 cm^{-1} peak becomes the strongest peak. Three peaks at 2910, 2979 and 3037 cm^{-1} become less well resolved and the peaks at 2038 and 464 cm^{-1} disappear with larger dosages (figure 5b-c).

3.3 $^{13}CD_3COOH$ adsorption on Pt(111) at 168K

The isotopically labeled molecule $^{13}CD_3COOH(D)$ has been studied with three relative exposures of 0.31, 1.25 and 3.75. The HREEL spectra are shown in figure 6a-c. At low dosages, peaks are observed at 225, 428, 661, 768, 903, 1049, 1176, 1388, 1602, 1902, 2058, 2203 and 2261 cm^{-1} (figure 6a). With larger dosages, the peaks at 428, 1902 and 2058 cm^{-1} disappear (figure 6b-c). The strongest peak is at 388 cm^{-1} with low dosage (figure 6a) and at 661 cm^{-1} with larger dosages (figure 6b-c).

4. Discussion

4.1 Acetic acid dosage vs. surface coverage at 168K

In figure 1, the Auger peak intensity ratio for C_{273}/Pt_{273} is plotted out as a function of increasing CH_3COOH dosage. A slope change has been observed at a relative exposure of 1.0. After this point, the C_{273}/Pt_{237} ratio grows very slowly with CH_3COOH dosage. This can be understood as follows. The CH_3COOH dosage below 1.0 is in the first monolayer coverage region so that the CH_3COOH molecules have high sticking probabilities due to the chemical interaction between the acetic acid adsorbate and the Pt(111) substrate. At about an exposure of 1.0, a monolayer of CH_3COOH is formed on the surface. After this point, the CH_3COOH molecules have lower sticking probabilities due to the weak van der Waals interaction between the acetic acid and the acetic acid covered substrate. This is indicated by a very slow increase of the $C_{(273)}/Pt_{(237)}$ peak to peak ratio as a function of dosage. The high slope region corresponds to a chemisorption process while the small slope region corresponds to a physisorption process. The difference in adsorption nature is the cause for the change in sticking probabilities and thus, for the change of the slope in figure 1.

In our acetic acid adsorption experiments, the adsorption temperature of 168K is a little high for physisorbed multilayers to be stable which is observed from our TDS experiments [12]. The possible electron beam induced desorption has been considered during Auger data collection and efforts have been made to reduce this effect by using a relatively low beam voltage (1kV) and a low filament emission current (0.5 mA). With these electronic parameters the current measured at the crystal is ~4 μA. However, the nature of the bonding that changes the acetic acid sticking probability will not be altered given the presence of the electron beam induced desorption process. In our latter discussion, a coverage of θ=1.0 will refer the point at which this dramatic change of slope in figure 1 is obtained. If we assume a sticking probability of CH_3COOH molecules for chemisorption

to be one and 1 langmuir ($1x10^{-6}$ torr.sec) as the monolayer exposure, we estimate that our doser for acetic acid adsorption has a pressure enhancement factor of about 125. This CH_3COOH dosage and the surface coverage correlation is further supported by HREELS results. In figure 2f, the acetic acid dosage is 1.25 which is a little over monolayer exposure and the lattice mode of multilayer acetic acid at 219 cm^{-1} is observed. Below this dosage, we have not observed this mode which agrees that at 1.25 dosage multilayer starts to form. This mode for larger dosages is hard to detect due to the broadened elastic peak and its high background tail which interferes strongly with this low frequency mode at 219 cm^{-1}.

4.2 Acetate formation on Pt(111) at 168K

As we can see from figure 2, at low acetic acid dosage (θ~0.2), the adsorption of CH_3COOH is dissociative. This is characterized by the lack of O-H related modes such as the stretching vibrational mode (υ_{OH} is at 3640 cm^{-1} for CH_3COOH monomer[13]), O-H in plane bending mode (δ_{OH} is at 1176 cm^{-1} for CH_3COOH monomer [13]) as well as O-H out of plane bending mode (γ_{OH} is 650 cm^{-1} for CH_3COOH monomer [14]). The absence of these O-H bond related vibrational modes in the HREEL spectra strongly suggests that the O-H bond of the acetic acid molecule is cleaved upon adsorption on Pt(111) at 168K, resulting in the acetate formation on Pt(111). The acetate species has also been identified for oxygen pre-exposed Pt(111) by Avery[6] in which it was intended to generate acetate species by enhancing the Bronsted basicity of the metal surface with pre-adsorption of oxygen. Our results indicate that even without oxygen preadsorption, the Pt surface has enough basicity to react with acetic acid forming surface acetate. The acetate species has also been reported by Chen et. al. on Al(111)[11], by Bowker et al. on Cu(110) [10] and by Sexton on Cu(111)[7-8].

The comparison of the vibrational frequencies of the acetate species is given in table 1 in which our result and the results from aqueous solution, Al(111), Cu(100) and oxygen preadsorbed Pt(111) are listed. The assignments for surface acetate vibrational

modes on Pt(111) at 168K are as follows: C-H stretching (υ_{CH}) at 2988~2930, symmetric COO stretching (υ_{sCOO}) at 1398 cm^{-1}, CH umbrella bending mode (δ_{CH_3}) at 1340 cm^{-1} (resolved from υ_{sCOO} mode at 1398 cm^{-1} with off-specular observation figure 4b), C-C stretching (υ_{CC}) at 1000 cm^{-1}, in plane COO bending (δ_{COO}) mode at 671 cm^{-1} and substrate platinum-oxygen of the acetate stretching vibration (υ_{Pt-O}) at 302 cm^{-1} . The strong intensity for υ_{sCOO}, δ_{COO} and υ_{Pt-O} in the specular direction indicates that these modes are dipole active. The absence of υ_{aCOO} in the specular spectra (figure 2a-c) indicates that this vibrational mode is dipole forbidden on the metal surface. This could be accounted for by an adsorption configuration of a bidentate acetate $\eta^2_{(O,O)}$-CH_3COO which is in a Cs symmetry. As explained by Sexton[7-8] and Chen et. al.[11], this configuration would give υ_{sCOO}, δ_{COO} and υ_{Pt-O} modes large dynamic dipole components perpendicular to the plane of the metal surface and hence strong on-specular peak intensities. The υ_{aCOO} vibrational mode, however, will be weak since its dynamic dipole has little component perpendicular to the plane of the metal surface. These are consistent with the surface dipole selection rule i.e. only those vibrations with a non-zero dynamic dipole component perpendicular to the plane of metal surface will be observed with dipole scattering. The off-specular scattering is known to enhance the impact scattering mechanism. The υ_{CH} and δ_{CH_3} peaks are examples here. The spectra shown in figure 4b indicates that the υ_{CH} mode at 2900-3000 cm^{-1} and the δ_{CH_3} mode at ~1340 cm^{-1} are enhanced by off-specular observation. These two modes are thus considered to be impact scattering enhanced.

Apart from the acetate formation as discussed above, further dissociation of CH_3COOH to $CO_{(a)}$ is observed as well. In figure 2a-b, υ_{CO} and υ_{Pt-CO} are observed at 2057 cm^{-1} and 467 cm^{-1}, respectively. These two peaks disappear for larger dosages (figure 2c-e). The small peak at ~413 cm^{-1} in figures 2e-g is the out of plane bending mode of the COO group (ρ_{COO}) in molecularly adsorbed acetic acid molecules. The formation of the adsorbed CO is clearly from the dissociation of CH_3COOH rather than from the chamber background CO adsorption since no such modes are observed prior to

CH_3COOH adsorption. Our temperature dependent HREELS and thermal desorption results also indicate that CO is a direct dissociation product from CH_3COOH at elevated temperatures[12]. The presence of a $CO_{(a)}$ fragment from CH_3COOH dissociation hints that further bond scission other than the O-H bond is possible at this adsorption temperature of 168K. Apparently, the C-C bond and C-O bond are broken to form $CO_{(a)}$. We have ruled out the presence of $HCOO_{(a)}$ and $CH_{3(a)}$ species. For the $HCOO_{(a)}$ species, the literature indicates that the υ_{sCOO} mode is in the range of 1330-1350 cm^{-1} [15-22] while the $CH_3COO_{(a)}$ species has υ_{sCOO} at 1398-1470 cm^{-1}[6-8, 11]. This is about 100 cm^{-1} higher than the corresponding mode in $HCOO_{(a)}$. The δ_{COO} mode is at 760-785 cm^{-1} for the $HCOO_{(a)}$ species while the $CH_3COO_{(a)}$ species has δ_{COO} at 650-675 cm^{-1} which is about 100 cm^{-1} lower than the corresponding mode in $HCOO_{(a)}$. The lack of a δ_{sCH_3} vibration, which has been reported to be a strong mode at ~1200 cm^{-1} for $CH_{3(a)}$ [23-24], indicates that the surface $CH_{3(a)}$ species is possibly not stable in our experimental conditions. The surface $CH_{2(a)}$ group has been reported on Ru(001)[25] with strong peaks at 2940 (υ_{sCH_2}) and 1450 cm^{-1} (δ_{sCH_2}). In figure 2b, modes at 2930, 2988 and 1398 cm^{-1} may have contributions from surface $CH_{2(a)}$ species. $CH_{(a)}$ species may also present since this species gives υ_{CH} modes at 3050 cm^{-1} and δ_{CH} mode at 770 cm^{-1}[26-27]. We have observed weak peaks at 2988 cm^{-1} and 768 cm^{-1} (figure 2a,b) which could be from $CH_{(a)}$. The peak at 768 cm^{-1} in figure 2a is also present with $^{13}CD_3COOH(D)$ adsorption at low dosage (figure 6a), which indicates that apart from the possible $CH_{(a)}$ other species may have contributions to this peak. The most probable one is $O_{(a)}$ since this species is also a counter part of $CO_{(a)}$ from CH_3COOH dissociative adsorption, and on Pt(111) this mode has been observed at 750-800 cm^{-1} with Ca impurities[28]. Thus, we observe CH_3COOH dissociatively adsorbed on Pt(111) at low dosages forming surface acetate ($CH_3COO_{(a)}$)and surface $H_{(a)}$. Acetate species could further decompose to $CO_{(a)}$, $O_{(a)}$ and CH_x species with x=1-2 at very low acetic acid dosage.

4.3 Molecular adsorption of acetic acid on Pt(111) at 168K

Non-dissociative molecular adsorption of acetic acid occurs after the Pt(111) surface is passivated by the species from acetic acid dissociation. When the acetic acid dosages exceed θ~0.5 new features of the vibrational spectra grow in at 932 cm^{-1} for CH_3COOH/Pt(111) (figure 2d-h) and at 913 cm^{-1} for $^{13}CD_3COOH(D)$/Pt(111) (figure 6b-c). With more exposure, the peak intensity increases and exceeds the δ_{COO} mode (~678cm^{-1}) as the second dominant peak (figure 2d-h). The width of this peak also increases as a function of increasing dosage. All these phenomena are not observed for deuterium substituted OH group molecule CH_3COOD in figure 5a-c. Thus, we conclude that peaks at 932 cm^{-1} for CH_3COOH adsorbate and 913 cm^{-1} for $^{13}CD_3COOH(D)$ adsorbates are related to the hydroxyl group (OH). After literature studies it turns out that this peak originates from the out of plane bending mode for the OH group (γ_{OH}) from acetic acid cyclic dimers which we will discuss in detail later. We would like to point out here that due to the strong hydrogen bonding between neighboring acetic acid molecules and possibly between acetic acid and acetate species, the υ_{OH} mode is no longer characteristic for molecular adsorption identification. The "free" OH stretching frequency (υ_{OH}) for the acetic acid molecule in the gaseous state at 430K is observed at 3583 cm^{-1} [29]. It decreases to a broad peak near 2900 cm^{-1} in the acetic acid crystal near 90K[29] and is hard to differentiate from the C-H stretching peak which also falls in this region. The υ_{OH} can vary from 2900 to 3100 cm^{-1} for liquid CH_3COOH with temperature and solvents due to their influence on the strength of hydrogen bonding[30]. It is thus not surprising that different υ_{OH} frequencies have been reported in the literature. However, the γ_{OH} mode is found to be characteristic [31] and thus is used here as a indicator of the presence of molecular adsorption. The γ_{OH} mode is observed with a dosage of θ~0.5 (figure 2d). With the presence of the γ_{OH} mode at ~932 cm^{-1}, the peak in the 2900-3020 cm^{-1} region becomes broadened (figure 2d-g) which we assume is due to contributions from $\upsilon_{H\text{-}O\text{-}H}$ in this region. On the Al(111)

surface $\upsilon_{H\text{-}O\text{-}H}$ has been observed at 2740 cm^{-1} for multilayer CH_3COOH adsorption[11]. The asymmetric shape in figure 2g at 2917 cm^{-1} with a shoulder at 2958 cm^{-1} and the off-specular spectra shown in figure 3 leads us to tentatively assign those peaks above 2950 cm^{-1}, at large dosages, as the $\upsilon_{H\text{-}O\text{-}H}$ mode since $\upsilon_{C\text{-}H}$ is believed to be enhanced in off-specular scattering which is observed below 2950 cm-1 in figure 3. However, as we have mentioned above, the assignment for this mode is not conclusive.

Comparing the coverage dependent HREEL spectra of CH_3COOH(figure 2), CH_3COOD (figure 5) and $^{13}CD_3COOH$(D) (figure 6), we have assigned the 1034 cm^{-1} band in figure 2, the 1039 cm^{-1} band in figure 5 and the 1039 cm^{-1} band in figure 6 to a C-C stretching vibration. The alternative assignment of this band to out-of-plane CH_3 bending (ρ_{CH_3}) [32] or OH in plane bending (δ_{OH}) [13] dose not seem appropriate here since this peak does not show a significant shift upon deuteration of either the methyl or the hydroxyl group.

The band at ~1660 cm^{-1} (figure 2d) is very weak in intensity. This mode is not detected for small dosages (figure 2a-c). The acetic acid isotope adsorptions have not resulted in significant shifts of this peak. For CH_3COOD adsorption, this band is at 1631-1660 cm^{-1} and for $^{13}CD_3COOH$ adsorption, this band is at 1600-1640 cm^{-1}. Thus, we can rule out a hydrogen related vibration for this band. A possible assignment for this band is from the carbonyl stretching mode ($\upsilon_{C=O}$) of the acetic acid dimers since with low dosages where the surface is dominated by acetate species, this mode is not detected (figure 2a-c). When the acetic acid dosages exceed the dimer formation range (θ~0.5) this mode is observed in on-specular scattering (figure 2d-h, figure 5a-c and figure 6b-c). A carbonyl stretching mode at ~1660 cm^{-1} has also been reported by Bellamy et. al.[30] which supports our assignment.

Strong bands at ~1400 cm^{-1} for CH_3COOH (figure 2d-h), at ~1388 cm^{-1} for CH_3COOD (figure 5a-c) and at ~1383 cm^{-1} for $^{13}CD_3COOH$(D) have two sources of contribution. At small dosages where acetate species dominate the surface, this band corresponds to υ_{sCOO} mode of the acetate species. At large dosages where both

acetate and acetic acid dimers are present, δ_{CH_3} mode of the acetic acid can also contribute to this peak. We consider that υ_{sCOO} mode of the acetate species is the major contributor for this peak due to the lack of isotope shift of this band when methyl group is substituted by D.

Table 2 has summarized the mode assignments for molecularly adsorbed acetic acid. Our peak assignments and those of gas phase acetic acid [13] and acetic acid adsorbed on Al(111) [11] are listed as well.

4.4 Hydrogen bonding and acetic acid dimerization

In the introduction, we have mentioned our motivation for the study of acetic acid adsorption on Pt(111). Our previous studies of hydrogen bonding effects were conducted on formamide ($HCONH_2$) on Ni(111)[4] and on Pt(111)[5]. In the $HCONH_2$/Ni(111) system, hydrogen bonding has been considered to influence the adsorption geometry of the formamide molecules which leads to two parallel reaction channels. For the $HCONH_2$/Ni(111) and $HCONH_2$/Pt(111) systems, red shifts and broadening of the υ_{NH} peak are observed and a dimer form of $HCONH_2$ was proposed. In this work for the acetic acid /Pt(111) system, we also observed strong hydrogen bonding between adsorbed acetic acid species which is indicated by the presence of a substantially blue shifted γ_{OH} mode of the dimer form of acetic acid.

Hydrogen bonding in the liquid and solid phase has been extensively studied[33]. However, not much attention has been given to hydrogen bonding effects in surface adsorption and surface reactions. Apart from the $HCONH_2$/Ni(111) and CH_3COOH/Pt(111) systems in which hydrogen bonding effects are focused, Key et. al.[34] have studied H_2O, HF,and NH_3 adsorption. They have observed that hydrogen bonding could shift sub-monolayer TDS peaks to higher temperatures and could change the order of the desorption kinetics. Since surface chemistry mostly concerns the first monolayer of adsorbed species, the hydrogen bonding in the first monolayer appears to be more important than the hydrogen bonding formed in multilayers which is

physisorption in nature and in many ways similar to the solid phase of the molecule. In our studies, the onset of γ_{OH} mode at 932 cm^{-1} appears at θ~0.5. This mode is significantly blue shifted ($\Delta\upsilon$~282 cm^{-1}) from the corresponding peak of the monomer (~650 cm^{-1}) and thus is assigned as the dimer γ_{OH} mode. This mode from the dimer form of different carboxylic acid molecules has been extensively studied as indicated in the literature (3, 4, 29, 31, 35, 36). The relative intensity of the γ_{OH} mode (relative intensity to the elastic peak of incident electron beam) as a function of dosage is plotted in figure 7. From this plot, it is deduced θ~0.3 is the onset of surface hydrogen bond formation. On deuteration of the hydroxyl group, the γ_{OD} mode falls into the δ_{COO} peak region as shown in figures 5b-c in which the peak at 687 cm^{-1} becomes the strongest peak with large CH_3COOD dosages. We consider that the peak at 687 cm^{-1} has contributions from two sources. One is the δ_{COO} mode and the other is the γ_{OD} mode. Without the contribution of the latter, υ_{sCOO} at ~1398 cm^{-1} would always be the dominant peak with all dosages as is seen for CH_3COOH molecules (figures 2a-h). The strongest peak of $^{13}CD_3COOH(D)$ adsorption in figure 6b-c is also at ~661 cm^{-1} which is expected since 57 atom% D composed for the hydroxyl group. Also, the deuteration on methyl group has removed the δ_{CH_3} contribution to the 1383 cm^{-1} band and thus the 1383 to 661 cm^{-1} peak intensity ratio is reduced.

The characteristic γ_{OH} mode for acetic acid dimers has been correlated to the strength of the hydrogen bonding energy[14] and the OH···O bond length[31]. From our results of γ_{OH} at ~932 cm^{-1} using this correlation we can estimate that the hydrogen bond strength ΔH to be ~7.3 kcal/mole (referenced to monomer γ_{OH} at 650 cm^{-1}[14]) and the $R_{O....O}$ distance to be ~2.68Å.

The presence of adsorbed monomer of acetic acid is not likely since for monomer the υ_{OH} mode should be at ~3583 cm^{-1} and γ_{OH} mode should be at ~650 cm^{-1}[14]. Neither of these modes is observed in our experiment.

4.5 Off-specular scattering and the dimer form of acetic acid

The surface selection rule indicates that a large perpendicular dynamic dipole component will give a strong peak in specular scattering (dipole scattering). The peak intensity would decrease dramatically as a function of off-specular scattering angle. The υ_{CO} peak has been accepted as exhibiting a dipole scattering mechanism [37]. Figure 8 plots out the variation of υ_{sCOO}, δ_{COO} and υ_{CH} peak intensities relative to the υ_{CO} peak intensity as a function of off-specular angle when all of these modes are present for CH_3COOH adsorption. It can be seen that as the off-specular angle increases, the υ_{sCOO} and δ_{COO} peak intensities drop even faster than that of the υ_{CO} peak indicating that δ_{COO} and υ_{sCOO} peaks are dominated by dipole scattering. The υ_{CH} peak shows intensity enhancement relative to the υ_{CO} peak with increasing off-specular angle suggesting that the υ_{CH} peak is dominated by the impact scattering mechanism. This is consistent with the general conclusion that the υ_{CH} mode has a property of off-specular enhancement [37]. Figure 9 is a plot of both γ_{OH} and υ_{CH} peak intensities relative to the dipole dominant υ_{sCOO} peak intensity as a function of off-specular angle. The decrease of γ_{OH} peak vs. υ_{sCOO} peak intensity ratio with off-specular scattering angle indicates that OH out of plane bending mode is also dominated by dipole scattering. This implies that the OH bending motion should have a strong perpendicular dynamic dipole component. In figure 10, we propose a cyclic dimer form of acetic acid adsorption configuration. This dimer form has the dimer ring nearly parallel to the metal surface and would thus give a strong perpendicular dynamic dipole component for OH out of plane bending motion. The C-C bond is tilted from the surface normal which agrees with the weak on-specular υ_{CC} peak (~1035 cm^{-1}) and possibly the weak on-specular CH bond related modes. This configuration can also account for the presence of a weak carbonyl stretching mode ($\upsilon_{C=O}$) at ~1660 cm^{-1} since the $\upsilon_{C=O}$ motion will give a non-zero but small perpendicular dynamic dipole component. The shift of the $\upsilon_{C=O}$ mode from 1717 cm^{-1} to 1660 cm^{-1} in the temperature dependent liquid CH_3COOH IR spectra has been

interpreted as a systematic change from the open chain form to the cyclic dimer form [30] which is consistent with our proposed cyclic dimer form of acetic acid adsorption. While a chain form of hydrogen bonded acetic acid is possible, the HREEL spectra of our experiment favor the cyclic dimer by comparison with the results of the known cyclic dimer IR spectra [30,31]. The onset of the dimer formation below monolayer coverage suggests that hydrogen bonding between the acetic acid molecule and acetate species is also possible, and the configuration of which would be similar to the cyclic dimer configuration in figure 10 with one of the H atom removed and all the rest of the configurations retained.

5 Summary

(1). CH_3COOH, CH_3COCD and $^{13}CD_3COOH$ adsorption on Pt(111) at 168K has been studied. The vibrational mode assignments are helped by isotope substitutions on both the methyl and the hydroxyl group of the acetic acid molecules leading to the mode assignments listed in table 1 and table 2.

(2). Acetic acid adsorption on Pt(111) at 168K exhibits both dissociative and non-dissociative adsorption. At very low dosage(θ~0.04), CH_3COOH dissociates into surface acetate species in an $\eta^2_{(O,O)}$-CH_3COO configuration. The acetate ion can further decompose into $CO_{(a)}$, $O_{(a)}$ and $CH_{x(a)}$ species with x=1-2.

(3) The acetate species ($CH_3COO_{(a)}$) is distinguishable from the formate species ($HCOO_{(a)}$) with their vibrational spectra. The former species has υ_{sCOO} mode at 1398~1470 cm^{-1} and δ_{COO} at 650~675 cm^{-1} while the latter species has υ_{sCOO} mode at ~100 cm^{-1} lower and the δ_{COO} mode at ~100 cm^{-1} higher than the corresponding mode for the former species.

(4). The onset of non-dissociative molecular adsorption of acetic acid at 168K is estimated to occur substantially at θ~0.4 which is below the monolayer coverage. It is characterized by the OH out of plane bending mode of acetic acid dimer at ~932 cm^{-1}.

(5). The hydrogen bonded dimer configuration is proposed which fits the HREEL spectra characteristics. The hydrogen bonding strength of the dimer ΔH is estimated to be ~7.3/kcal/mole and the $R_{(O\cdots O)}$ distance for hydrogen bonded dimer acetic acid is estimated to be ~2.68 Å.

Acknowledgements: This work was supported in part by the Office of Naval Research.

Figure Caption

Figure1. Acetic acid Auger uptake curve, the acetic acid adsorption temperature is 168K, the chamber background pressure is $5x10^{-10}$ torr when the dosing beam is on.

Figure 2. Coverage dependent HREEL spectra of CH_3COOH on Pt(111)

with acetic acid adsorption at 168K and dosages of (a) θ~0.03 (b) θ~0.19

(c) θ~0.30 (d) θ~0.50 (e) θ~0.63 (f) θ~1.25 (g) θ~2.5 (h) θ~7.5

Figure 3. Off-specular spectra of CH_3COOH adsorption on Pt(111) at 168K with a dosage of θ~7.5

Off-specular angles are: (a) o degree (b) 3 degree (c) 5 degree (d) 10 degree

Figure 4. Off-specular spectra of CH_3COOH adsorption on Pt(111) at 168K with a dosage of θ~0.19 (a) on-specular (b) 5 degree off-specular

Figure 5. Coverage dependent HREEL spectra of CH_3COOD on Pt(111) with acetic acid dosages of (a) θ~0.63 (b) θ~1.25 (c) θ~3.75

Figure 6. Coverage dependent HREEL spectra of $^{13}CD_3COOH(D)$ adsorption on Pt(111) at 168K with acetic acid dosages of (a) θ~0.3 (b) θ~1.25 (c) θ~3.75

Figure 7. The relative intensity of the γ_{OH} mode as a function of the acetic acid dosage

Figure 8. The relative intensities of the υ_{sCOO}, δ_{sCOO} and υ_{CH} modes as a function of the off-specular angle

Figure 9. The relative intensity ratios of $\gamma_{OH}/\upsilon_{sCOO}$ and $\upsilon_{CH}/\upsilon_{sCOO}$ as a function of the off-specular angle

Figure 10. Proposed cyclic acetic acid dimer adsorption configuration

References

1. Robert T. Morrison, Organic chemistry, 4th edition, Allyn and Bacon Inc., p778, 1983

2. L. J. Bellamy, R. F. Lake and R. J. Pace, Spectrochimica, 19, 443, 1963

3. R. E. Jones and D. H. Templeton, Acta Cryst. 11, 484, 1958

4. Q. Gao, W. Erley, D. Sander, H. Ibach and J. C. Hemminger, J. Phys. Chem., in press

5. C. F. Flores, Q. Gao and J. C. Hemminger, Surf. Sci., in press

6. N. R. Avery, J. Vacuum Sci. Technol. 20, 592, 1982

7. B. A. Sexton, J. Vacuum Sci. Technol. 17, 141, 1980

8. B. A. Sexton, Chem. Phys. Letters, 65, 469, 1979

9. G. R. Schoofs and J. B. Benziger, Surf. Sci. 143, 359, 1984

10. M. Bowker and R. J. Madix, Appl Surf. Sci. 8, 299, 1981

11. J. G. Chen, J. E. Crowell and J. T. Yates, Jr.. Surf. Sci. 172, 733, 1986

12. TDS results show the onset of desorption from a multilayer film at dosing time of ~20 seconds under these experimental conditions.

13. R. C. Herman and R. Hofstadter, J. Chem. Phys. 6, 534, 1938 and 7, 460, 1939

14. M. Sh. Rosenberg, A. V. Iogansen, A. A. Mashkovsky, S. E. Odinokov, Spectroscopy Letters, 5, 75, 1972

15. J. E. Crowell, J. G. Chen and J. T. Yates, Jr., J. Chem. Phys., 85, 3111, 1986

16. R. J. Madix, J. L. Gland, G. E. Mitchell and B. A. Sexton, Surf. Sci. 125, 481, 1983

17. B. A. Sexton, Surf. Sci. 88,319, 1979

18. S. L. Miles, S. L. Bernasek and J. L Gland, Surf. Sci. 127, 271, 1983

19. N. R. Avery, B. H. Toby, A. B. Anton and W. H. Weinberg, Surf. Sci, 122, L574, 1982

20. B. A. Sexton and R. J. Madix, Surf. Sci. 105, 177, 1981

21. N. R. Avery, Appl. Surf. Sci., 11/12, 774, 1982 and 14, 149, 1982/83

22. P. Hofmann, S. R. Bare, N. V. Richardson and D. A. King, Surf. Sci. 133, L459, 1983

23. Y. Zhou, M. A. Henderson and J. M. White, Surf. Sci., 221, 160, 1989

24. M. B. Lee, Q. Y. Yang, S. L. Tang and S. T. Ceyer, J. Chem. Phys., 85, 1693, 1986

25. P. M. George, N. R. Avery, W.H. Weinberg and F. N. Tebbe, JACS, 105, 1393, 1983

26. J. E. Demuth and H. Ibach, Surf. Sci. 89, 425, 1979

27. M. B. Lee, Q. Y. Yang and S. T. Ceyer, J. Chem. Phys., 87, 2724, 1987

28. Kathryn G. Lloyd, PhD thesis, Univ. of Calif. Irvine, p148, 1986

29. M. Hauric, A. Novak, J. Chim. Phys., 62, 137, 1965; Structure and Bonding, Vol. 18, p180, Springer-Verlag, 1974

30. L. J. Ballamy, R. F. Lake and R. J. Pace, Spectrochimica Acta, 19, 442, 1963

31. Ingrid Fischmeister, Spectrochimica Acta, 20, 1071, 1964

32. K. Ito and H. J. Bernstein, Can. J. Chem., 34, 170, 1956

33. The Hydrogen Bond, P. Schuster, G. Zundel and C. Sandorfy ed. North-Holland Publishing Company, 1976 vol. 1-3

34. B. D. Kay, K. R. Lykke, J. R. Creighton and S. J. Ward, J. Chem. Phys., 91, 5120, 1989

35. D. Hadzi, B. Orel and A. Novak, Spectrochimica Acta, 29A, 1745, 1973

36. A. Novak, Structure and Bonding, Vol. 18, pp177, J. D. Dunitz Ed., Springer-Verlag, 1974

37. Electron Energy loss spectroscopy and surface vibrations, H. Ibach and D. L. Mills ed., Academic Press, 1982

38. M. Haurie and A. Novak, Spectrochimica Acta 21, 1217, 1965

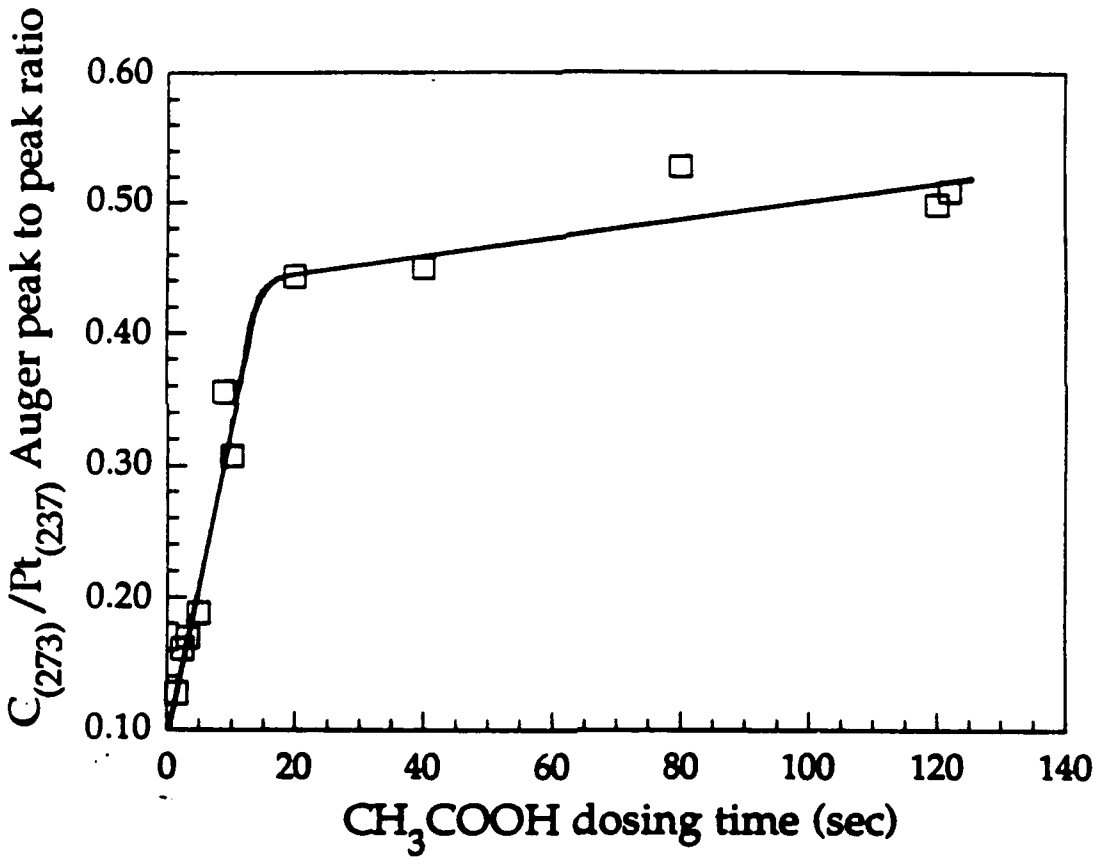
$C_{(273)}/Pt_{(237)}$ Auger peak to peak ratio
0.60
0.50
0.40
0.30
0.20
0.10
0
20
40
60
80
100
120
140
CH_3COOH dosing time (sec)

fig. 1

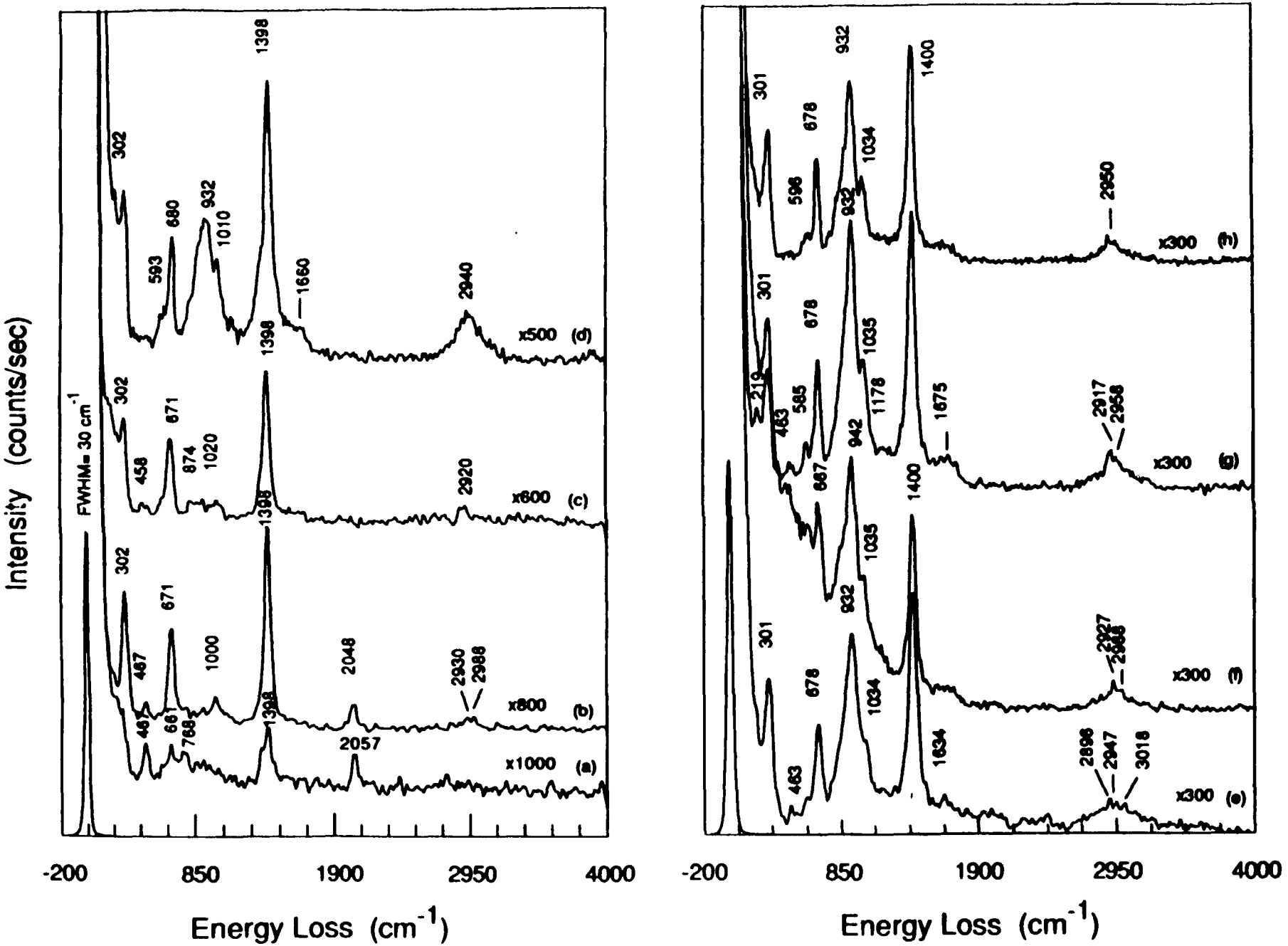
Intensity (counts/sec)
FWHM= 30 cm-1
302
593
680
932
1010
1398
1660
2940
x500 (d)
302
458
671
874
1020
1398
2920
x600 (c)
302
467
671
1000
1398
2048
2930
2988
x800 (b)
467
661
768
1398
2057
x1000 (a)
-200
850
1900
2950
4000
Energy Loss (cm-1)
301
596
678
932
1034
1400
2950
x300 (f)
301
219
483
585
678
942
1035
1178
1675
2917
2958
x300 (g)
301
667
932
1035
1400
x300 (h)
301
463
678
1034
1634
2896
2947
3018
x300 (e)
-200
850
1900
2950
4000
Energy Loss (cm-1)

fig 2.

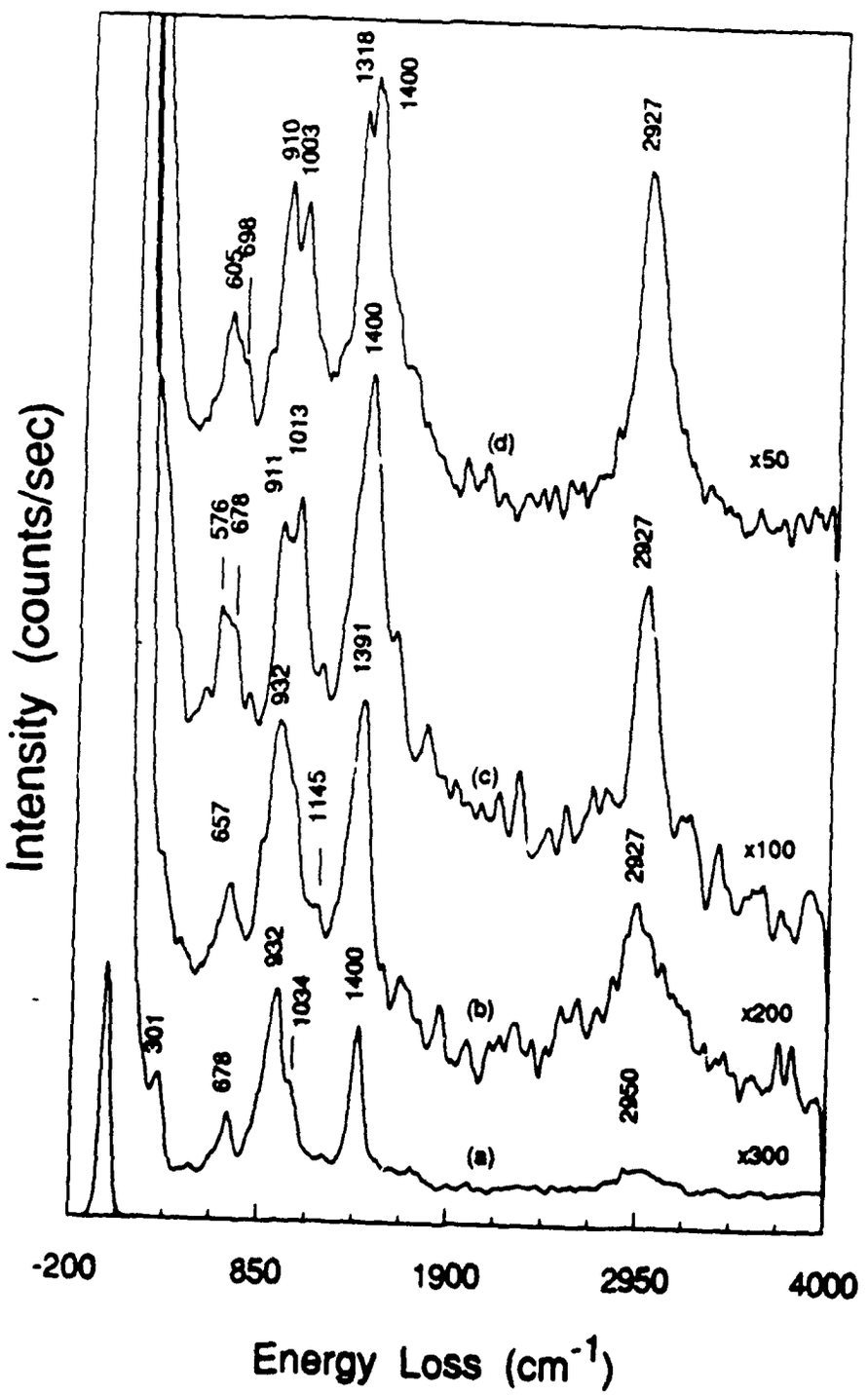
Intensity (counts/sec)
-200
850
1900
2950
4000
Energy Loss (cm^{-1})
(a)
x50
605
698
910
1003
1318
1400
1400
2927
(b)
x200
301
678
932
1034
1400
2927
2950
(c)
x100
657
1145
932
1391
2927
(d)
x50
576
678
911
1013
1400
2927

fig 3.

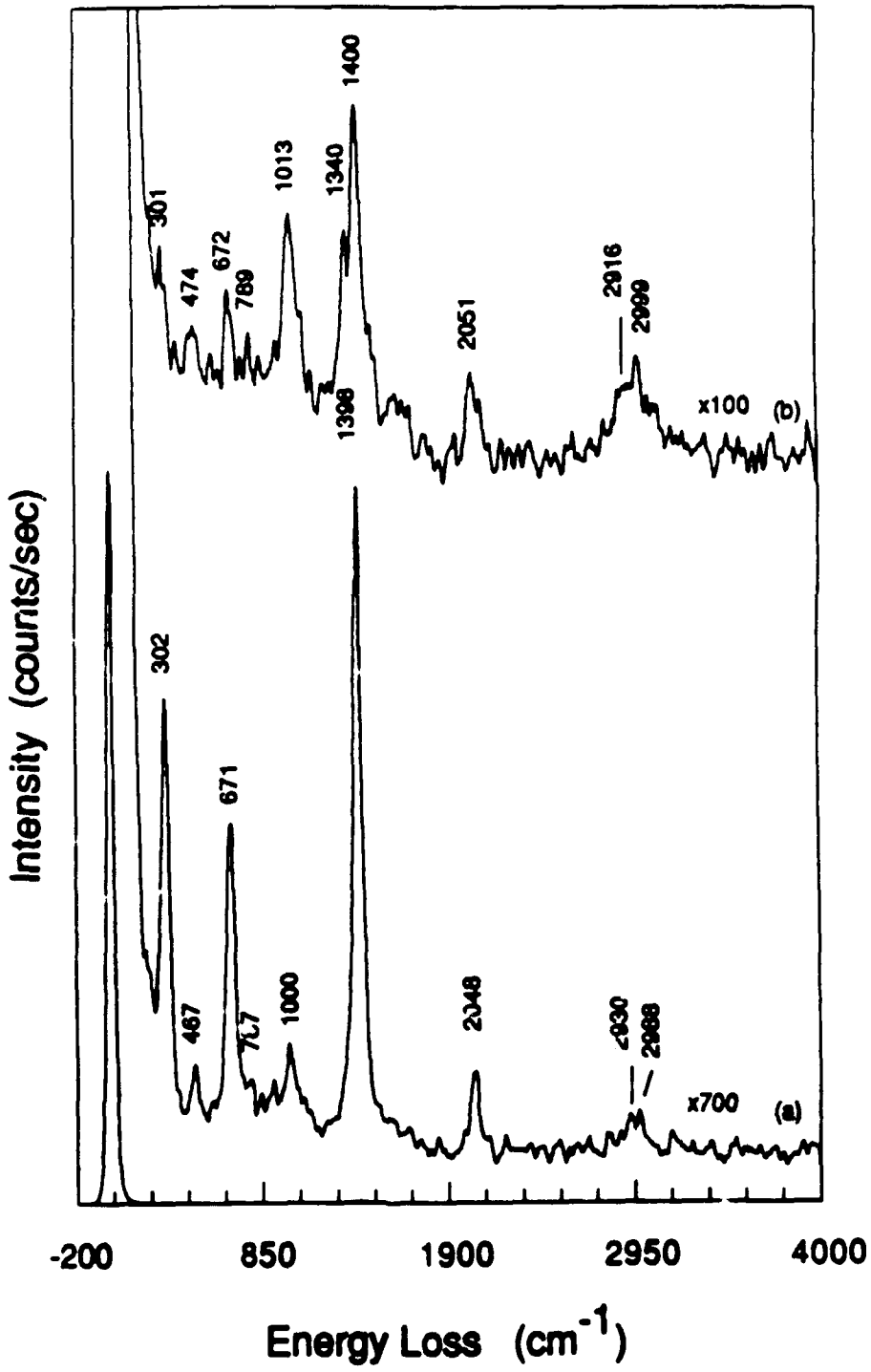
Intensity (counts/sec)
-200
850
1900
2950
4000
Energy Loss (cm-1)
301
474
672
789
1013
1340
1400
1398
2051
2916
2999
x100
(b)
302
467
671
717
1000
2048
2930
2988
x700
(a)

fig. 4

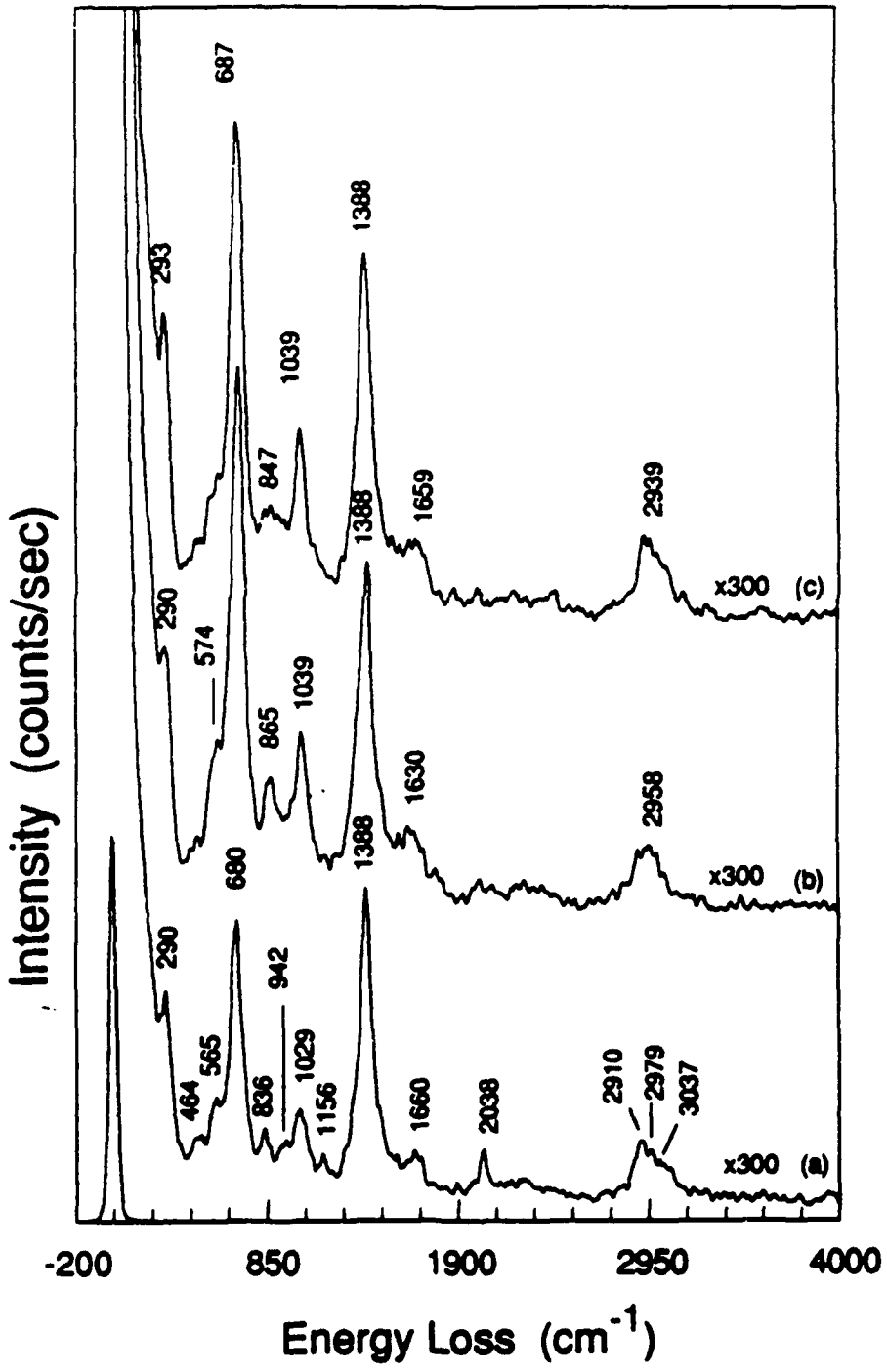
Intensity (counts/sec)
687
293
1388
1039
847
1388
1659
2939
x300
(c)
290
574
865
1039
1630
2958
x300
(b)
680
290
942
565
464
836
1029
1156
1660
2038
2910
2979
3037
x300
(a)
-200
850
1900
2950
4000
Energy Loss (cm-1)

fig. 5

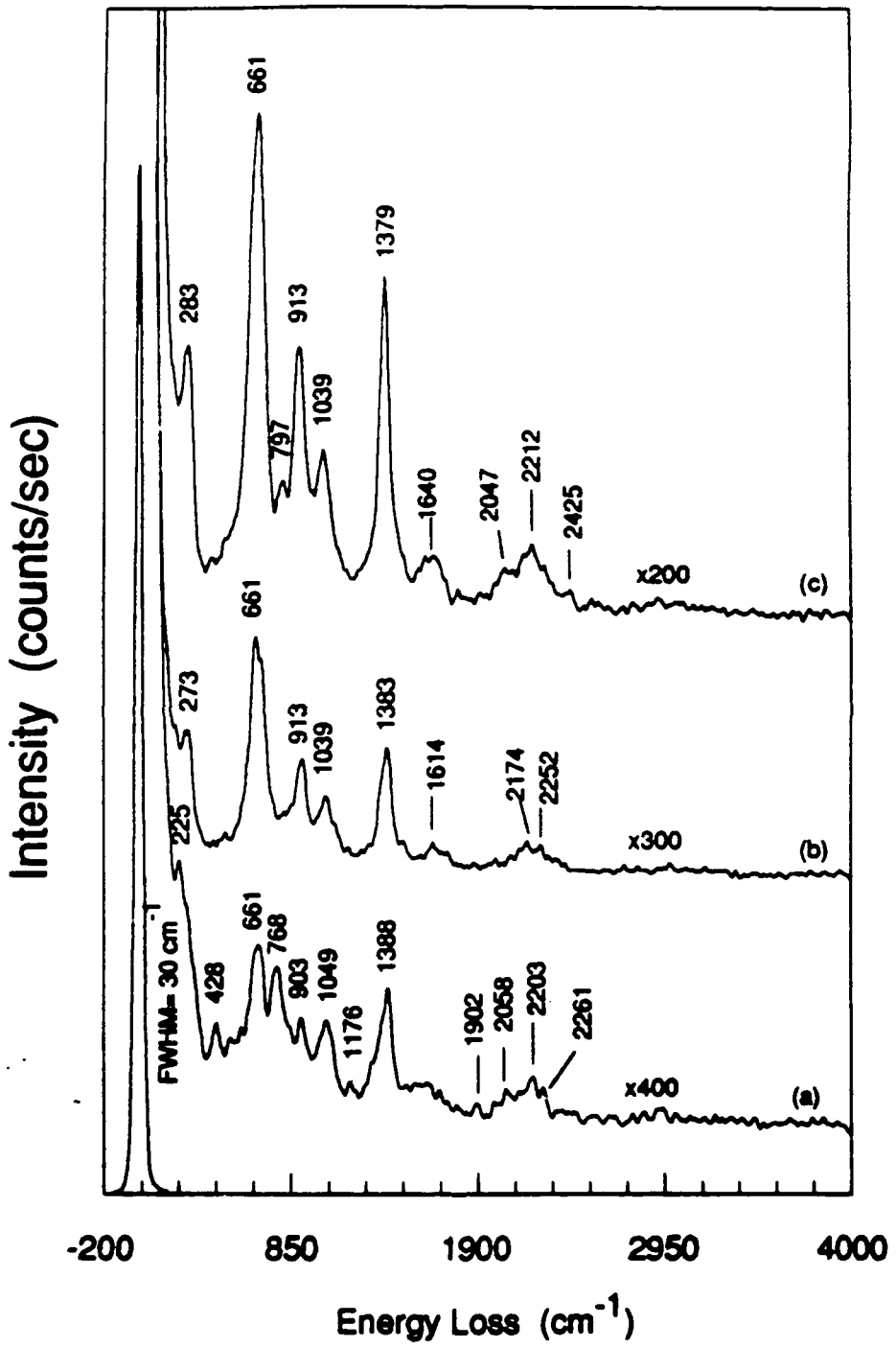
Intensity (counts/sec)
661
283
913
1379
797
1039
1640
2047
2212
2425
x200
(c)
661
273
913
1039
1383
225
1614
2174
2252
x300
(b)
661
768
428
903
1049
1388
1176
1902
2058
2203
2261
FWHM= 30 cm-1
x400
(a)
-200
850
1900
2950
4000
Energy Loss (cm-1)

fig 6.

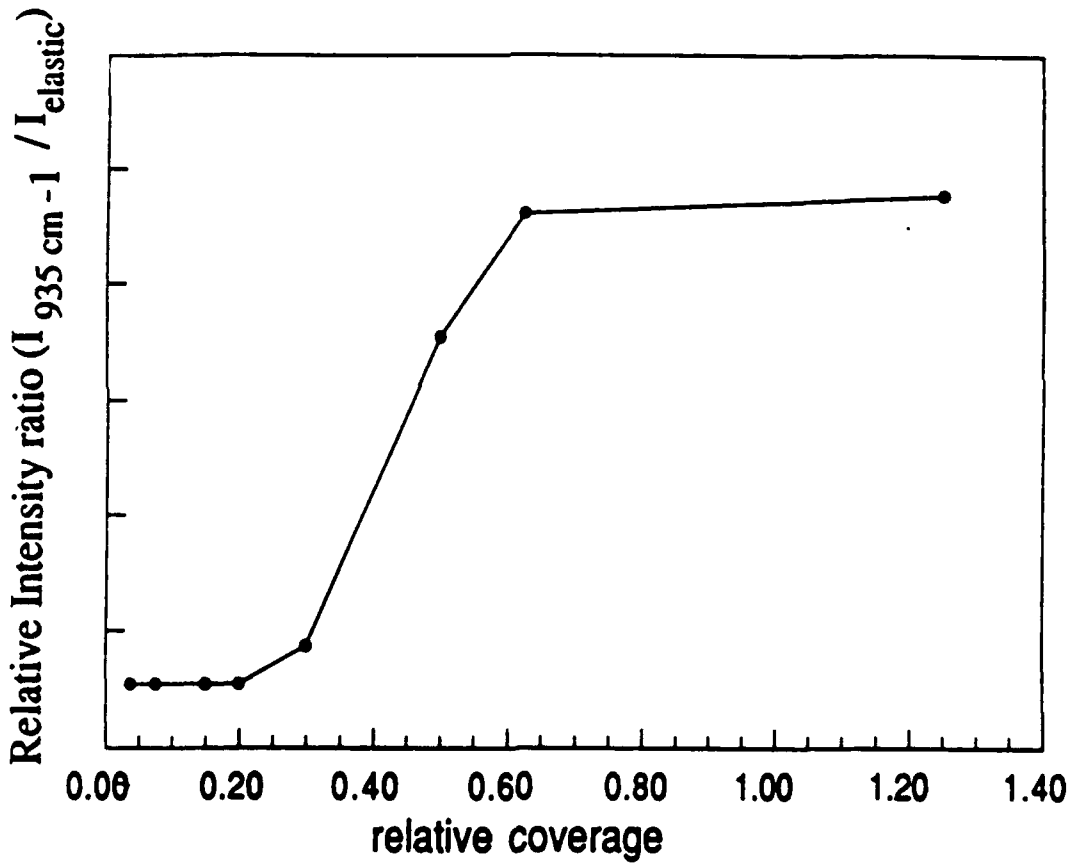
Relative Intensity ratio ($I_{935\ cm-1}$ / $I_{elastic}$)
0.00
0.20
0.40
0.60
0.80
1.00
1.20
1.40
relative coverage

fig. 7

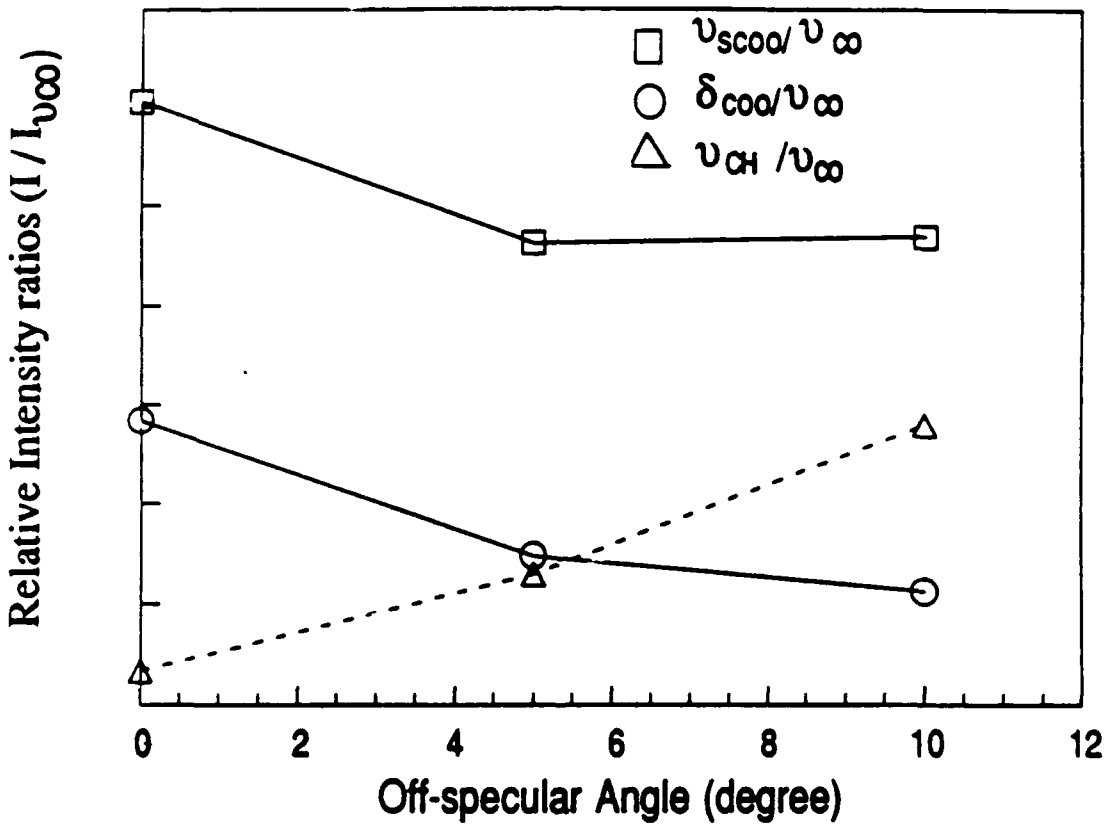
Relative Intensity ratios (I / I$_{\upsilon\infty}$)
$\upsilon_{SCOO}/\upsilon_{\infty}$
$\delta_{COO}/\upsilon_{\infty}$
$\upsilon_{CH}/\upsilon_{\infty}$
0
2
4
6
8
10
12
Off-specular Angle (degree)

fig. 8

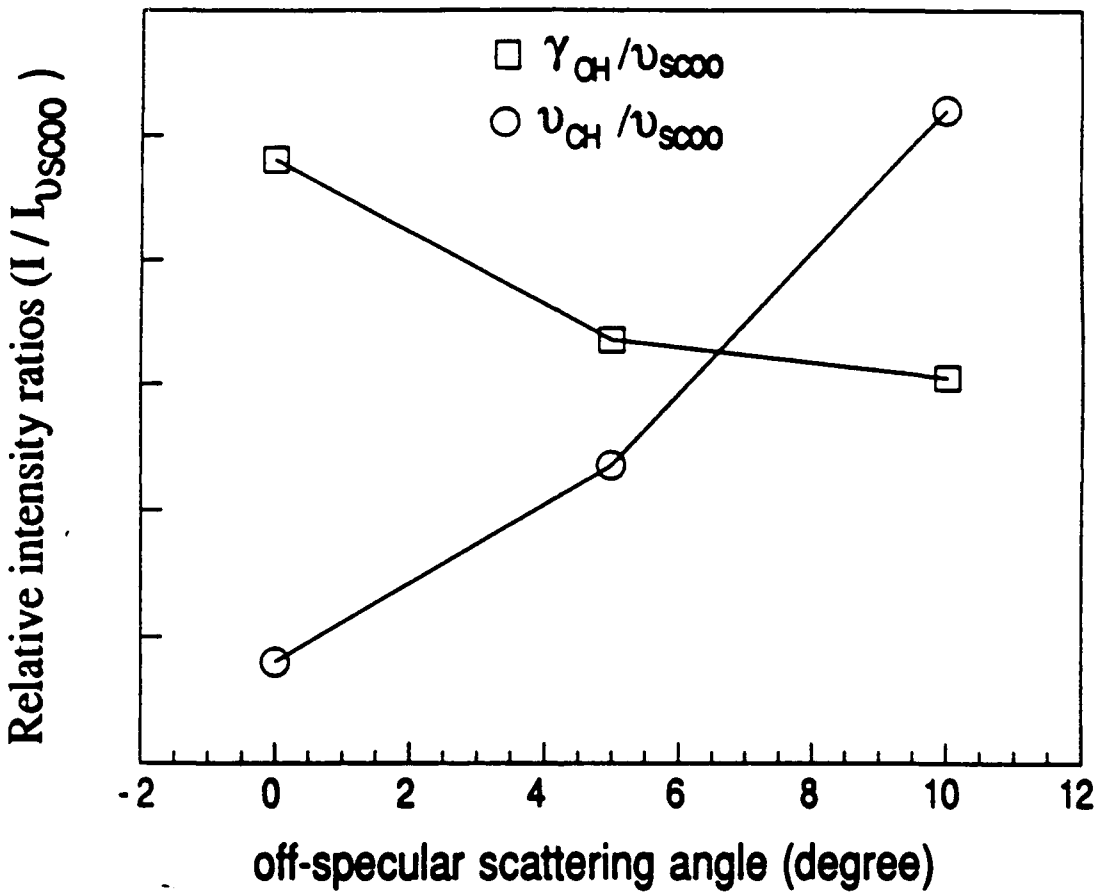
□ $\gamma_{CH}/\upsilon_{SCOO}$
○ $\upsilon_{CH}/\upsilon_{SCOO}$
Relative intensity ratios ($I / I_{\upsilon SCOO}$)
-2
0
2
4
6
8
10
12
off-specular scattering angle (degree)

fig. 9

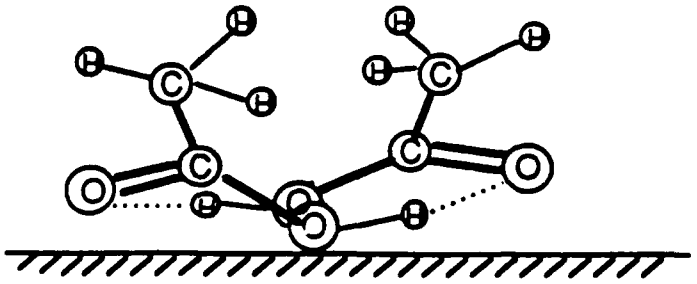

fig. 10

Table 1. Acetate Vibrational mode assignments

	CH_3COO^- [32]	(CD_3COO^-)	Cu(100) [8]		Al(111) [11]		Pt(111) [6]	Pt(111) [this work]	
υ_{CH}	2935	(2111)	3000	(2218)	3025	(2260)	—	2930 -2988	(2261, 2203)
υ_{aCOO}	1556	(1545)	—	—	—	—	—	—	—
υ_{sCOO}	1413	(1406)	1434	(1413)	1470	(1470)	1400	1398	(1388)
δ_{CH_3}	1344	(1085)	—	—	—	—	—	1340 os	(903)
υ_{C-C}	926	(883)	1041	(1061)	1055	(1070)	—	1000	(1049)
δ_{COO}	650	(619)	677	(648)	695	(655)	665	671	(661)
ρ_{COO}	471	(419)	—	—	—	—	—	463	(428)
υ_{M-O}	—	—	339	(308)	425	(410)	300	302	(225)

os: Off-specular observation

Table 2. Acetic Acid Vibrational mode assignments

	$CH_3COOH_{(g)}$ [32]	($CD_3COOH_{(g)}$)	$CH_3COOH_{(s)}$ [38]	($CD_3COOH_{(s)}$)	Al(111) [11]		Pt(111) [this work]	
υCH	3030	(2128)	—	(22780, 2116)	3030	(2275, 2155)	2927	(2252, 2174)
υOH	3125	(3100)	2875	(2852)	2740	(2740)	2988	(2425)
$\upsilon_{C=O}$	1739	(1730)	1648	(1641)	1730	(1730)	1675	(1640)
δ_{CH_3}	1387	(1075)	1439	(1035, 1055)	1400	(1050)	1400	(913)
υ C-O	1282	(1220)	1284	(1287)	1350	(1310)	1318 os	—
δOH	1186	(1156)	1418	(1404)	990	(945)	1176	(1176)
ρ_{CH_3}	—	—	1049	(920)	—	—	1034	(903)
υ_{C-C}	—	—	908	(856)	—	—	1034	(1039)
γ OH	—	—	923	(920)	—	—	932	(913)

os: Off-specular observation